# Spin-forbidden excitation of $[Ru(bpy)_3]^{2+}$ enables red light driven photocatalysis

Géraud Chacktas,[a][b] Taline Kerackian,[a][c] Björn Pfund,[d] Maud Villeneuve[b], Didier Durand[b], Nicolas Fabre[e], Céline Fiorini-Debuisschert[e], Oliver S. Wenger[d] and Eugénie Romero*[a]

[a] G. Chacktas, Dr. T. Kerackian, Dr. E. Romero
Département Médicaments et Technologies pour la Santé (DMTS), SCBM
Université Paris Saclay, CEA, INRAE
91191 Gif-sur-Yvette, France
E-mail: eugenie.romero@cea.fr

[b] G. Chacktas, Dr. M. Villeneuve, Dr. D. Durand
Drug Design Small Molecules Unit
Institut de Recherche et Développement Servier Paris-Saclay
91190 Gif-sur-Yvette, France

[c] Dr. T. Kerackian
CEA, DAM, Le Ripault
F-37260 Monts, France

[d] Dr. B. Pfund, Prof. O. S. Wenger
Department of Chemistry, University of Basel, St. Johanns-Ring 19
CH-4056 Basel, Switzerland

[e] Dr. N. Fabre, Prof. C. Fiorini
Université Paris Saclay, CEA, CNRS, SPEC
91191 Gif sur Yvette, France

**Abstract:** Red light driven catalysis presents a promising alternative to conventional blue light photocatalysis, offering enhanced light penetration, functional group tolerance, and energy efficiency. However, its widespread application remains underdeveloped, partly due to the lack of readily accessible photocatalysts. $[Ru(bpy)_3]^{2+}$ is one of the most frequently used blue light photocatalysts. Here, we demonstrate the application of $[Ru(bpy)_3]^{2+}$ in various red light-induced transformations and investigate the underlying photophysical properties, revealing a direct singlet-to-triplet excitation under red light irradiation. Our findings suggest that red light driven photocatalysis could be possible with many other photocatalysts not considered for this purpose until now.

**Introduction:** Over the last two decades, photocatalysis has emerged as a disruptive synthetic tool, providing privileged access to transformations that were previously arduous, thus becoming one of the fastest-growing fields in organic synthesis.[1,2] Photoredox catalysis has evolved as an attractive approach to facilitate various chemical reactions under relatively mild conditions. By light absorption, photocatalysis accesses unique single-electron radical chemistry, enabling unprecedented process efficiencies. The versatility of photoredox catalysis lies in its ability to activate a broad range of chemical functional groups. Particularly, blue light photocatalysis has opened broad applications owing to the availability of many suitable photocatalysts.[3-13]

However, numerous applications in organic synthesis and large-scale industrial facilities suffer from practical limitations from UV/visible light catalysis; i) Upscaling reactions to process and development scale remains challenging because of the low penetration depths of visible light in reaction media. Flow chemistry offers an alternative to this issue.[14,15] Unfortunately, a systematic re-optimization is often required to translate a reaction from batch to flow chemistry; ii) The use of UV/Visible light is often energetically uneconomical, as most of the photon's energy is dissipated into thermal energy; iii) The use of high energy photons can lead to reduced functional group tolerance, limiting its applications.[10] Especially since most molecules of interest absorb UV/visible light, which further restricts light penetration depths and can eventually lead to unwanted side reactions. As a result, photoredox catalysis remains challenging to transpose into process development. Hence, exploring alternatives for UV/visible light driven photoredox catalysis could lead to more specific, selective, and robust reactions, thereby developing the chemical and pharmaceutical industries by addressing scientific and technical challenges.

Red light driven photocatalysis can overcome the limitations of UV/visible light photocatalysis.[16] Such low-energy light allows deeper penetration into the reaction media and facilitates milder reaction conditions, leading to higher functional group tolerance. However, this research field is still in its infancy. Consequently, very few photocatalytic systems have been described using red light.[17-23]

The rare number of reported photocatalysts (PCs) capable of facilitating important transformations under red light irradiation underscores the need for new PCs for red light photocatalysis. As a response, new PCs have been reported, most of which are photocatalytic oxidants. Both organic and organometallic compounds have been successfully used in red light driven photocatalysis.[17-23] Among organometallic PCs, ruthenium complexes have shown particular promise and have been extensively used in UV/visible photocatalysis. Ru(polypyridyl)-type catalysts are leaders of this complex family, with countless transformations using $[Ru(bpy)_3]^{2+}$ (bpy = 2,2'-bipyridine) as a photocatalyst.[13] $[Ru(bpy)_3]^{2+}$ has chemical and photophysical properties suitable for photocatalysis, such as chemical and conformational stability and a long-lived excited state (~1 µs). Furthermore, $[Ru(bpy)_3]^{2+}$ is a highly versatile PC, capable of generating both strong reducing species ($[Ru(bpy)_3]^{2+}$/ $[Ru(bpy)_3]^{+}$ = –1.33 V vs SCE in MeCN) and strong oxidant species ($[Ru(bpy)_3]^{3+}$/ $[Ru(bpy)_3]^{2+}$ = +1.29 V vs SCE in MeCN).[13]
Recently, Sun et al. described a group of ruthenium polypyridyl complexes such as $[Ru(bpyvp\text{-}OMe)_3]^{2+}$ (bpyvp-OMe = bis-4-methoxystyryl-2,2'-bipyridine) possessing two-photon absorption (TPA) properties upon 740 nm light irradiation (Figure 1).[24] These chromophores were applied in new low-energy initiated photoredox catalysis, bioimaging, and photodynamic therapy by generating singlet oxygen. However, such TPA processes typically require high power density light sources for excitation.[25]

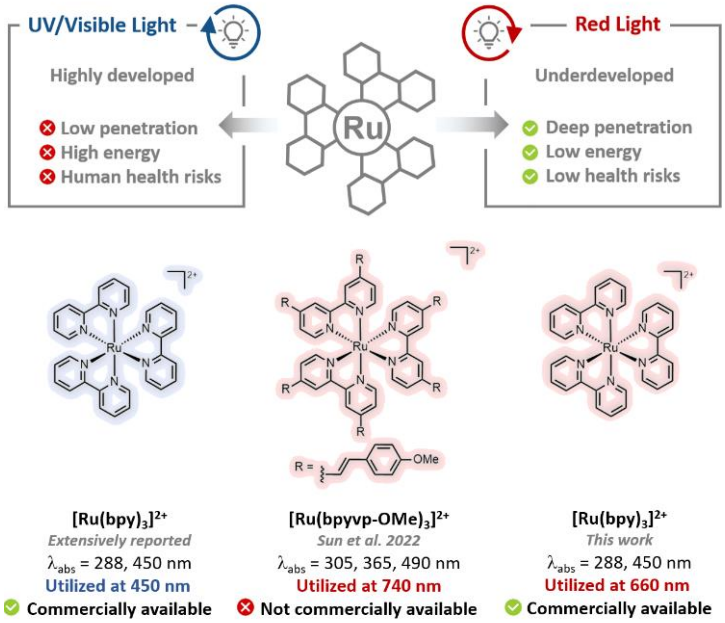


**Figure 1.** Comparison between UV/Visible and red light photocatalysis, and different ruthenium polypyridyl complexes.

Inspired by these results, we have recently investigated the ability of various ruthenium-based chromophores to catalyze various reactions under red light irradiation (730 nm) by High-Throughput Experimentation (HTE).[26-28] Among other ruthenium complexes, $[Ru(bpy)_3]^{2+}$ was screened as a potential negative control, as $[Ru(bpy)_3]^{2+}$ is not known to absorb above 550 nm. Serendipitously, we observed catalytic activity using $[Ru(bpy)_3]^{2+}$ under red light irradiation.
Therefore, we investigated the unexpected reactivity by optimizing an aza-Henry coupling reaction under red light photocatalysis using HTE. We report a range of red light induced photocatalysis using $[Ru(bpy)_3]^{2+}$. The subsequent mechanistic investigations suggest a direct singlet to triplet excitation when irradiating $[Ru(bpy)_3]^{2+}$ above 600 nm. This direct singlet-triplet excitation bypasses the intersystem crossing (ISC), enhancing the overall energy efficiency.[29] Such minimized energy losses are particularly important when using low energy red light to preserve the necessary redox power for effective photocatalysis.[30]
In this paper, we demonstrate that the commercially available $[Ru(bpy)_3]^{2+}$ can serve as an efficient catalyst for red light photocatalysis, in addition to its well-established performance under blue light. Our study also suggests re-evaluating previously dismissed photocatalysts, as advances in direct singlet-triplet excitation reveal their potential for effective red light use.

**Results and discussion:** We have initially investigated the ability of different ruthenium complexes to catalyze oxidative reactions under red light irradiation. The initial benchmark reaction studied was an aza-Henry reaction between nitromethane and 2-phenyl-1,2,3,4-tetrahydroisoquinoline **1**. In the first assays, the aza-Henry reaction was carried out in the presence of different PCs, with nitromethane as the solvent, under 730 nm light irradiation.[31]

Among the photocatalysts evaluated, $[Ru(bpy)_3]^{2+}$ was screened as a potential negative control, as no conversion was expected. Surprisingly, $[Ru(bpy)_3]^{2+}$ showed a non-negligible yield of 20% (isolated yield). This result was highly unexpected as no absorption bands beyond 550 nm are reported for $[Ru(bpy)_3]^{2+}$.[13] Hence, we investigated this intriguing result with a new HTE campaign focused on $[Ru(bpy)_3]^{2+}$ as a PC (Figure 2a). The aza-Henry reaction was evaluated using two different $[Ru(bpy)_3]^{2+}$ photocatalysts with different counterions, i.e. $Ru(bpy)_3(PF_6)_2$ and $Ru(bpy)_3Cl_2•6H_2O$.[32] Photocatalyst loading (1 mol%, 5 mol%, and 10 mol%), equivalents of nitromethane (1 or 10 equiv.), solvents (DMSO, MeCN, THF, and $CHCl_3$), and irradiation wavelength (420 nm and 730 nm) were screened, resulting in 96 different conditions. Over the whole well plate, the following results were obtained: i) Using 10 equivalents of nitromethane provided better results than using 1 equivalent; ii) $Ru(bpy)_3Cl_2•6H_2O$ with a catalytic charge of 10 mol% is the most efficient catalytic system; iii) DMSO was identified as the best-performing solvent; iv) Irradiation with 730 nm light resulted in higher yields compared to 420 nm irradiation. The unexpectedly low yields observed under blue LED irradiation can be attributed to the significant formation of side and degradation products. This phenomenon is likely favored by the extensive irradiation time and the high photon energy. This indicates that switching from blue to red light could impact the selectivity of the reaction when using $[Ru(bpy)_3]^{2+}$. As 1, 5, and 10 mol% catalytic charges resulted in good yields, a systematic study was performed (see SI, Section S1.2). Although 1 and 5 mol% catalytic loading resulted in the formation of the desired product, the reaction duration of up to 5 days was unsatisfactory. A catalytic loading of 10 mol% reduced the reaction time to 48 h and was identified as the best compromise between reaction time and yield. After identifying the optimal reaction conditions using HTE, the reaction was reproduced in batch. Under 660 nm irradiation, compound **1** reacted with 10 equivalents of nitromethane in presence of 10 mol% of $Ru(bpy)_3Cl_2•6H_2O$ in DMSO for 40 hours to give the expected product with an isolated yield of 53% (Figure 2b).

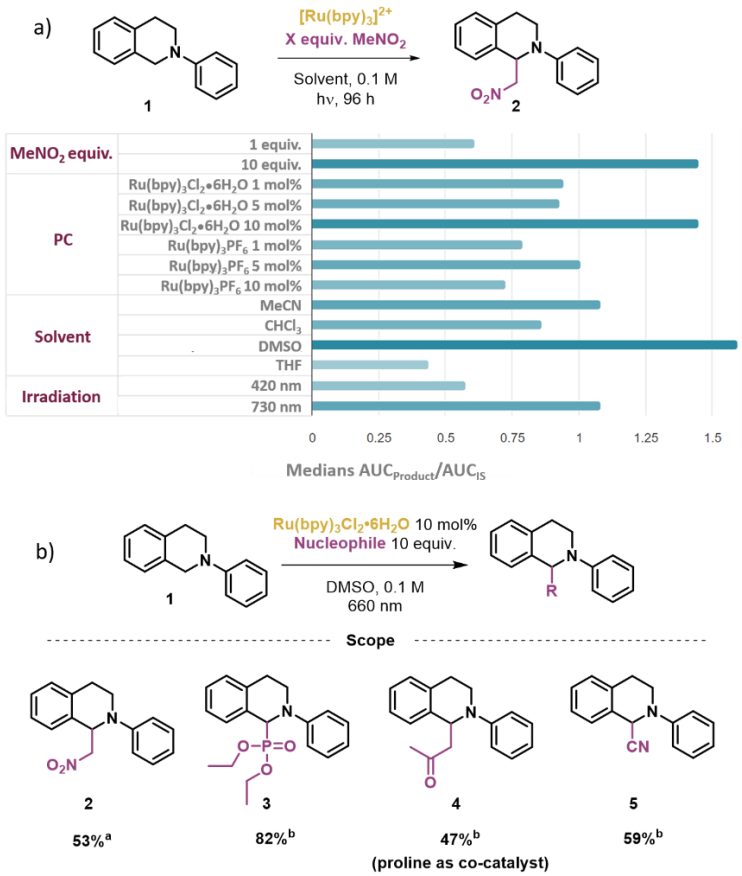


**Figure 2.** a) Optimization of photocatalyzed aza-Henry reaction via HTE campaign (96 well plate). Results are expressed as medians of the Area Under the Curve (AUC) of the product against the AUC of the internal standard (IS) obtained via UPLC analysis. b) Scope of nucleophiles in the aza-Henry reaction under red light. [a] Reaction performed during 40 h; [b] Reaction performed during 48 h.

To confirm the applicability of the process, we evaluated other nucleophiles, including diethyl phosphite, acetone, and trimethylsilyl cyanide (Figure 2b). All desired products were isolated with decent yields, demonstrating the reaction tolerance to several functional groups. The control experiment without a photocatalyst or a light source for the formation of compound **2** showed no product formation, confirming the photocatalytic activity of $[Ru(bpy)_3]^{2+}$.

With these promising results in hand, we then focused on extending the scope of possible catalytic transformations under red light using $[Ru(bpy)_3]^{2+}$ as the photocatalyst (Figure 3). Among the reactions performed, the hydroxylation of (4'-isopropoxy-[1,1'-biphenyl]-4-yl)boronic acid resulted in 4'-isopropoxy-[1,1'-biphenyl]-4-ol **6** with 51% yield.[33] The reduction of α-bromoketone afforded the corresponding ketone **7** in 78% yield.[34] The cycloaddition between dimethyl aniline and *N*-methylmaleimide allowed the formation of the corresponding hydroquinoline structure **8** in 68% yield.[35] The oxidative cyclization of thiobenzamide proved efficient under our conditions to afford thiadiazole **9** in 68% yield.[36] Activating $[Ru(bpy)_3]^{2+}$ with red light in dual metallaphotoredox catalysis produced ethyl 4-(piperidin-1-yl)benzoate **10** in 77% yield from the coupling of bromoarene and piperidine using $[Ru(bpy)_3]^{2+}$ and $NiBr_2$.[37] This underlines the ability of $[Ru(bpy)_3]^{2+}$ to catalyze, under red light irradiation, essential reactions such as a C-N cross coupling. In addition, the challenging α-arylation of cyclohexanone with aryl iodide was performed, affording the desired compound **11** with a 47% yield.[38] Control experiments were systematically performed (without PC or light irradiation), resulting in minor or no product formation. Notably, these transformations were performed without any further optimization, following conditions described in literature.

$[Ru(bpy)_3]^{2+}$ is typically described with a 1 mol% catalytic loading in blue light driven catalysis. Here, the dual metallophotoredox catalysis reaction leading to **10** and the α-arylation of cyclohexanone reaction affording **11** prove that several red light photocatalyzed reactions require relatively low catalytic loading. However, the aza-Henry oxidation shows a drastic correlation between conversion and catalytic loading, requiring 10 mol% PC for most reactions. To examine a more sustainable approach, we investigated a recycling strategy that allows multiple uses of the photocatalyst. Hence, we supported 26.7 µmol of $Ru(bpy)_3Cl_2•6H_2O$ on 1 g of silica, preventing the photocatalyst's leaching over time.[39] We first evaluated the reproducibility of the cycloaddition between dimethylaniline and *N*-methylmaleimide leading to compound **8** (Figure 3) under red light with $Ru(bpy)_3Cl_2•6H_2O@SiO_2$ as a heterogeneous photocatalyst. The presence of silica slightly lowers the reaction efficiency, probably because of light scattering, but results in comparable yields (see SI, Section S4.1). The recyclability of $Ru(bpy)_3Cl_2•6H_2O@SiO_2$ was then tested on the same reaction under red light irradiation in four successive runs, with no reduction of the reaction efficiency observed. Hence, $Ru(bpy)_3Cl_2•6H_2O@SiO_2$ appears to be a sustainable solution to compensate for the relatively high catalytic loading required.

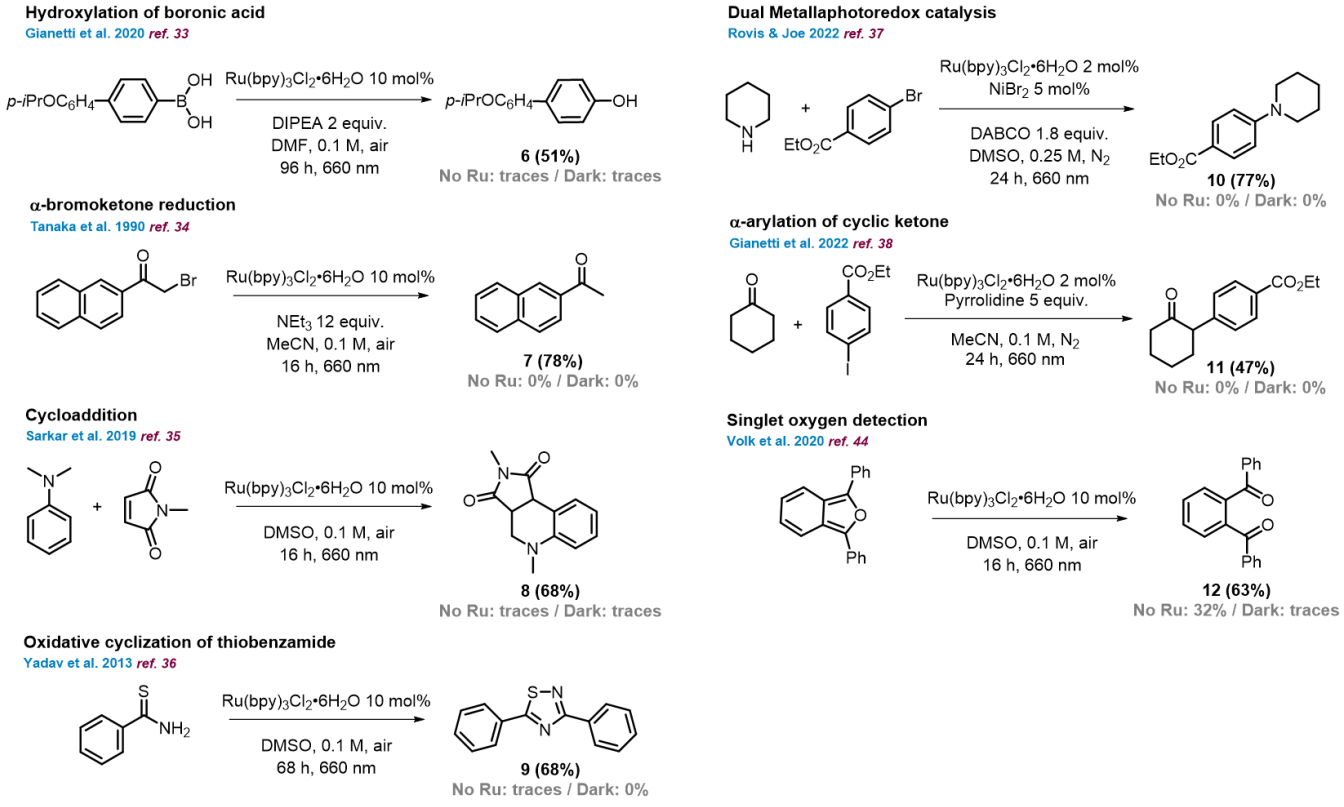


**Figure 3.** Scope of reactions catalyzed by $Ru(bpy)_3Cl_2·6H_2O$ under red light. Isolated yields are indicated in brackets.

All previously described transformations involve the reductive quenching of the excited $[Ru(bpy)_3]^{2+}$ photocatalyst forming $[Ru(bpy)_3]^{+}$. As $[Ru(bpy)_3]^{2+}$ is well described as a versatile photocatalyst under blue light irradiation because of its oxidative and reductive excited state potentials ($E_{1/2}([Ru(bpy)_3]^{3+}/^{3*}[Ru(bpy)_3]^{2+})$ = -0.81 V vs. SCE, $E_{1/2}(^{3*}[Ru(bpy)_3]^{2+}/[Ru(bpy)_3]^{+})$ = +0.77 V vs. SCE) and its triplet energy of 2.12 eV, different reaction mechanisms

were investigated, including oxidative quenching and energy transfer catalysis (see Figure S3). However, no reactivity (or degradation) was observed for reactions involving an oxidative quenching mechanism, even though those reactions are known to occur under blue light irradiation. This observation can potentially be explained by the lower cage escape probability when using low-energy photons.[40-43]
In contrast, the energy transfer mechanism was successfully demonstrated using red light by generating singlet oxygen (Figure 3), which facilitates the oxidation of diphenyl benzofuran to form 1,3-dibenzoylbenzene **12**.[44]
Given the unexpected reactivity of $[Ru(bpy)_3]^{2+}$ under red light irradiation, mechanistic investigations were conducted.

**Mechanistic insights:** We confirmed the observed reactivity by reproducing the photocatalyzed reactions in another laboratory (see SI, Section S5.1). In addition, the influence of possible impurities such as $RuCl_3$, ruthenium oxide, ruthenium black, and bipyridine under red light irradiation was evaluated. However, these impurities did not provide a reliable explanation for the observed red light driven photocatalysis (see SI, Section S5.2).
Further, the used light irradiation system was investigated. Commonly used LEDs are often described as monochromatic light systems. In reality, the emission spectrum generally shows a tailing on both ends of the main emission band. The emission spectra of our LED irradiation systems were obtained from each supplier. Both LEDs from Kessil lamps PR and Lumidox system from Analytical Sales and Services, emit light down to 600 nm (see SI, Section S5.3). Such tailing can potentially explain the observed reactivity and the need for high catalytic loading. Therefore, we reproduced the oxidative cyclization of thiobenzamide to thiadiazole **9** (Figure 3) using a 645 longpass filter to ensure the absence of high energy photons (see SI, Section S5.4). When using the 645 nm longpass filter, comparable product formation confirmed the photoactivation of $[Ru(bpy)_3]^{2+}$ under red light irradiation.
Additionally, we investigated the possibility of a two-photon absorption mechanism under red light irradiation, a phenomenon previously observed in some ruthenium-based complexes.[24] First, the aza-Henry reaction leading to compound **2** was performed with the light power varied from 5 to 100%. The observed yields appear to be linearly correlated to the light power, indicating a monophotonic process (Figure 4a). Second, the emission intensity of $[Ru(bpy)_3]^{2+}$ at 700 nm was investigated upon 640 nm laser excitation at different laser powers (Figure 4b). The same experiment was conducted using a 660 nm pulsed laser, varying the pulse energy between 5 to 140 µJ per pulse and detecting the gated emission spectra of $[Ru(bpy)_3]^{2+}$ immediately after pulse excitation (see SI, Section S5.5). Both experiments indicate a linear correlation between the emission intensity and the excitation energy, pointing to a monophotonic absorption process of $[Ru(bpy)_3]^{2+}$ under these irradiation conditions.

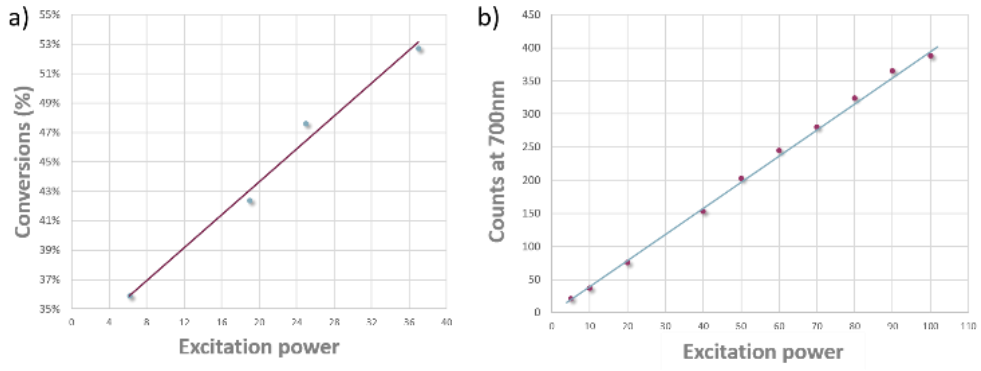


**Figure 4.** a) Evolution of the conversion of the aza-Henry oxidation reaction (in DMSO at 0.1 M, under 660 nm for 40 h) as a function of light excitation power. b) Evolution of the emission intensity at 700 nm as a function of the excitation power at 640 nm with a bandpass filter at 700 nm ± 10 nm.

Because neither the starting materials nor $[Ru(bpy)_3]^{2+}$ possess an intense absorption band above 550 nm (see SI, Section S1.4), and two-photon absorption has been excluded, the observed photoactivity upon red light excitation remains intriguing. Some studies show that the photocatalyst might aggregate with the starting material, forming an electron donor-acceptor (EDA) complex. Such EDA complexes can cause bathochromic shifts that extend the absorption band further into the red spectroscopic region.[45,46] However, in our developed catalytic systems, no bathochromic shift of the $[Ru(bpy)_3]^{2+}$ absorption band (or the rise of any other absorption band) was observed in the presence of the starting materials or different solvents (see SI, Section S5.4).
Because of the necessity of relatively high PC loading for several developed catalytic systems, we investigated the UV/visible absorption spectra of $[Ru(bpy)_3]^{2+}$ in DMSO at high concentrations (5 mM) up to 850 nm (Figure 5a). According to early work investigating Ru(II) doped $[Zn(bpy)_3]Br_2$ at 8 K,[47] the electronic origin for the lowest spin-forbidden charge transfer state of $[Ru(bpy)_3]^{2+}$ is near 18000 $cm^{-1}$ (550 nm). In our UV/visible spectra obtained in

DMSO at room temperature, absorption features were observed tailing to considerably longer wavelengths (Figure 5a). This indicates a solvatochromatic effect that shifts the absorption band further into the red part of the spectrum compared to solid state. This observed absorption band tail is located in the same spectral range as the room temperature phosphorescence emission of $[Ru(bpy)_3]^{2+}$ originating from the radiative decay of the triplet metal-to-ligand charge transfer ($^3$MLCT) excited state back to the ground state (Figure 5b, black trace).[48] Taken together, these findings suggest that the absorption band tail in Figure 5a corresponds partially to vibronic spin-forbidden singlet-to-triplet ($S_0 \rightarrow T_1$) transitions,[49] i.e., transitions from vibrational levels of the electronic ground state to the lowest $^3$MLCT state.

To verify our assignment further, we conducted a gated emission study at a high $[Ru(bpy)_3]^{2+}$ concentration in DMSO using excitation wavelengths above 610 nm up to 660 nm, where only direct $S_0 \rightarrow T_1$ transition is expected. All gated emission spectra were recorded immediately after the pulse excitation and time-integrated over 2 µs. The obtained emission spectra were normalized, revealing only minor differences between the reference spectrum of $[Ru(bpy)_3]^{2+}$ (Figure 5b, black trace) obtained upon 450 nm excitation and the emission spectra of $[Ru(bpy)_3]^{2+}$ (Figure 5b, purple trace) after excitation above 610 nm. The minor variations observed on the higher energy side of the emission band (at 550 nm) are attributed to inner filter effects caused by the high concentration of $[Ru(bpy)_3]^{2+}$. A similar study was performed using steady-state emission spectroscopy with green (532 nm) and red (633 nm) laser excitation (Figure S59). The resulting emission signals were normalized, and similar to the gated emission spectra (Figure 5b), both spectra superimpose perfectly. Therefore, we attribute the observed absorption band to a direct $S_0 \rightarrow T_1$ excitation band, similar to what has been described for isoelectronic osmium(polypyridyl)-type photocatalysts. These catalysts exhibit direct $S_0 \rightarrow T_1$ transitions with higher molar absorption coefficients of ~1000 $M^{-1}$ $cm^{-1}$ owing to stronger spin-orbit coupling.[50-56]

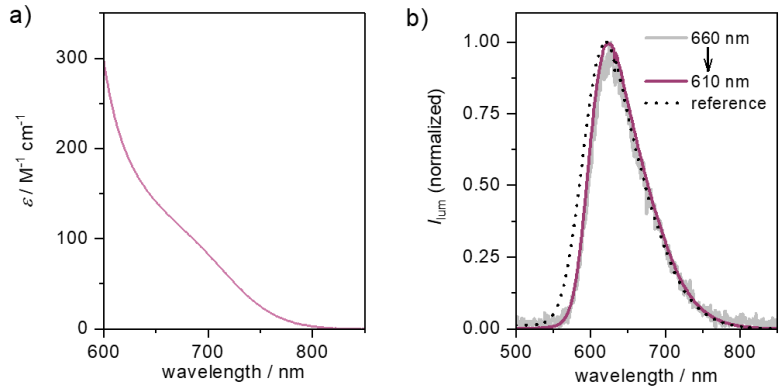


**Figure 5.** a) Calibrated red tail of the UV/visible absorption spectrum of $[Ru(bpy)_3]^{2+}$ in DMSO at 22 °C. b) Normalized time-gated luminescence spectra of 5 mM $[Ru(bpy)_3]^{2+}$ in air-saturated DMSO at 20 °C upon excitation between 660 nm and 610 nm (grey to purple traces). The normalized reference spectrum (black dotted line) was obtained using a $1 \times 10^{-5}$ M solution of $[Ru(bpy)_3]^{2+}$ in air-saturated DMSO at 20 °C upon excitation at 450 nm. All gated emission spectra were recorded immediately after the excitation and integrated over 2 µs. The differences between the reference spectrum and the observed emission spectra upon red light excitation are owed to filter effects of the highly concentrated $[Ru(bpy)_3]^{2+}$ solution.

In summary, our studies point to a weak spin-forbidden but non-negligible absorption of $[Ru(bpy)_3]^{2+}$ in the red light region, leading to a monophotonic absorption mechanism of $[Ru(bpy)_3]^{2+}$ under red light irradiation.

Despite the diverse applications of direct singlet-to-triplet excitation in sensitized triplet-triplet upconversion, photocatalysis, and phototherapy for osmium-based complexes and the widespread use of ruthenium-based photocatalysts, the phenomenon remains underexplored for ruthenium-based systems.[57] Hence, this study may serve as a starting point for exploring direct singlet-to-triplet excitation in ruthenium-based complexes or isoelectronic first-row transition metal complexes to design further red light induced applications.[58]

**Conclusion:** This paper describes how $[Ru(bpy)_3]^{2+}$ functions as an efficient photocatalyst under red light photoactivation. The photocatalyzed aza-Henry reaction was optimized using HTE, and compatibility with several nucleophiles was demonstrated. $[Ru(bpy)_3]^{2+}$ has been employed in various photocatalyzed reactions via a reductive quenching mechanistic pathway. We demonstrated the ability to immobilize $[Ru(bpy)_3]^{2+}$ on silica and recycle the photocatalyst, effectively reducing the overall catalytic cost. The unexpected photoactivity of $[Ru(bpy)_3]^{2+}$ under red light prompted investigations revealing a spin-forbidden excitation pathway. Our findings may pave the way for red light activated processes, using commercially available, stable, and widely implemented photocatalysts, allowing the exploration of a much larger scope.

## Supporting Information

The authors have cited additional references within the Supporting Information.

## Acknowledgements

G.C. is grateful to Servier Laboratories and Agence Nationale de la Recherche Technologique for PhD funding. T.K. is grateful for CEA DAM Le Ripault for post-doctoral fellow funding. The authors describe no conflict of interest. All authors thank the GIPSY team for the development of HTDesign software (Cyrille Petat and Pascal Drevet), used for Experiment Design and Data visualization in HTE campaigns. All authors thank Z. Amara and P. Atakpa for their help with photocatalysis process development. All authors warmly thank national and international researchers for exciting and fruitful discussions.

**Keywords:** Photocatalysis • High-Throughput Experimentation • Red-light irradiation • Spin-forbidden transition

References:

[1] P. Melchiorre, *Chem. Rev.* **2022**, *122*, 1483–1484.

[2] M. H. Shaw, J. Twilton, and D. W. C. MacMillan *J. Org. Chem.* **2016**, *81*, 16, 6898–6926.

[3] Y. Sakakibara, K. Murakami, *ACS Catal.* **2022**, *12*, 1857−1878.

[4] M. J. Genzink, J. B. Kidd, W. B. Swords, T. P. Yoon *Chem. Rev.* **2022**, *122*, 1654−1716.

[5] D. Lunic, E. Bergamaschi, C. J. Teskey *Angew. Chem., Int. Ed.* **2021**, *60*, 20594−20605.

[6] R. C. McAtee, E. J. McClain, C. R. J. Stephenson *Trends in Chemistry* **2019**, *1*, 111−125.

[7] L. Marzo, S. K. Pagire, O. Reiser, B. König *Angew. Chem., Int. Ed.* **2018**, *57*, 10034−10072.

[8] C. Michelin, N. Hoffmann *ACS Catal.* **2018**, *8*, 12046−12055.

[9] J. Twilton, C. Le, P. Zhang, M. H. Shaw, R. W. Evans, D. W. C. MacMillan *Nat. Rev. Chem.* **2017**, *1*, No. 0052.

[10] N. A. Romero, D. A. Nicewicz *Chem. Rev.* **2016**, *116*, 10075−10166.

[11] J. B. Bell, J. A. Murphy *Chem. Soc. Rev.* **2021**, *50*, 9540−9685.

[12] R. Brimioulle, D. Lenhart, M. M. Maturi, T. Bach *Angew. Chem., Int. Ed.* **2015**, *54*, 3872−3890.

[13] C. K. Prier, D. A. Rankic, D. W. C. MacMillan *Chem. Rev.* **2013**, *113*, 5322−5363.

[14] S. D.A. Zondag, D. Mazzarella, T. Noël *Annu. Rev. Chem. Biomol. Eng*. **2023**, *14*, 283–300.

[15] Z. J. Garlets, J.D. Nguyen, C. R. J. Stephenson *Isr. J. Chem.* **2014**, *54*, 351−360.

[16] A. H. Schade, L. Mei *Org. Biomol. Chem.* **2023**, *21*, 2472−2485.

[17] D. E. Yerien, M. V. Cooke, M. C. García Vior, S. Barata-Vallejo, Al Postigo *Org. Biomol. Chem.* **2019**, *17*, 3741–3746.

[18] J. Lee, J. W. Papatzimas, A. D. Bromby, E. Gorobets, D. J. Derksen *RSC Adv.* **2016**, *6*, 59269−59272.

[19] L. Mei, J. Moutet, S. M. Stull, T. L. Gianetti *J. Org. Chem.* **2021**, 86, 10640−10653.

[20] F. Glaser, O. S. Wenger *JACS Au* **2022**, *6*, 1488–1503.

[21] B. D. Ravetz, N. E. S. Tay, C. L. Joe, M. Sezen-Edmonds, M. A. Schmidt, Y. Tan, J. M. Janey, M. D. Eastgate, T. Rovis *ACS Cent. Sci.* **2020,** *6,* 11, 2053–2059.

[22] J. B. Bilger, C. Kerzig, C. B. Larsen, O. S. Wenger *J. Am. Chem. Soc.* **2021**, *143*, 1651−1663.

[23] N. Sellet, M. Cormier, J.-P. Goddard *Org. Chem. Front.* **2021**, *8,* 6783−6790.

[24] G. Han, G. Li, J. Huang, C. Han, C. Turro, Y. Sun *Nat. Commun.* **2022**, *13*, 2288.

[25] J. Karges, S. Kuang, F. Maschietto, O. Blacque, I. Ciofini, H. Chao, G. Gasser *Nat. Commun.* **2020**, *11*, 3262.

[26] M. Shevlin *ACS Med. Chem. Lett.* **2017***, 8*, 601–607.

[27] S. M. Mennen, C. Alhambra, C. L. Allen, M. Barberis, S. Berritt, T. A. Brandt, A. D. Campbell, J. Castañón, A. H. Cherney, M. Christensen, D. B. Damon, J. E. de Diego, S. García-Cerrada, P. García-Losada, R. Haro, J. M. Janey, D. C. Leitch, L. Li, F. Liu, P. C. Lobben, D. W. C. MacMillan, J. Magano, E. McInturff, S. Monfette, R. J. Post, D. Schultz, B. J. Sitter, J. M. Stevens, I. I. Strambeanu, J. Twilton, K. Wang, M. A. Zajac *Org. Process Res. Dev.* **2019**, *23*, 1213–1242.

[28] X. Caldentey, E. Romero *Chemistry – Methods* **2023**, e202200059.
[29] M. Hussain, S. S. Razi, T. Tao, F. Hartle *J. Photochem. Photobiol*. C **2023**, *56*, 100618.
[30] B. Pfund, V. Hutskalova, C. Sparr, O. S. Wenger *Chem. Sci.*, **2023**,*14*, 11180–11191.
[31] J. L. Clark, J. E. Hill, I. D. Rettig, J. J. Beres, R. Ziniuk, T. Y. Ohulchanskyy, T. M. McCormick, M. R. Detty *Organometallics* **2019**, *38*, 2431−2442.
[32] J. Zanzi, Z. Pastorel, C. Duhayon, E. Lognon, C. Coudret, A. Monari, I. M. Dixon, Y. Canac, M, Smietana, O. Baslé *JACS Au* **2024**, *8*, 3049–3057.
[33] L. Mei, J. M. Veleta, T. L. Gianetti *J. Am. Chem. Soc.* **2020**, *142*, 12056−12061.
[34] S. Fukuzumi, S. Mochizuki, T. Tanaka *J. Phys. Chem.* **1990**, *94*, 722−726.
[35] T. Mandal, S. Das, S. De Sarkar, *Adv. Synth. Catal.* **2019**, *361*, 3200–3209.
[36] V. P. Srivastava, A. K. Yadav, L. D. S. Yadav *Synlett* **2013**, 24, 465−470.
[37] S. L. Goldschmid, N. E. S. Tay, C. L. Joe, B. C. Lainhart, T. C. Sherwood, E. M. Simmons, M. Sezen-Edmonds, T. Rovis *J. Am. Chem. Soc.* **2022**, *144*, 22409−22415.
[38] M. M. Hossain, A. C. Shaikh, J. Moutet, T. L. Gianetti *Nat. Synth.* **2022**, *1*, 147–157.
[39] V. Blanchard, Z. Asbai, K. Cottet, G. Boissonnat, M. Port, Z. Amara *Org. Process Res. Dev.* **2020**, *24*, 822−826.
[40] C. Wang, H. Li, T.H. Bürgin, O. S. Wenger *Nat. Chem.* **2024**, *16*, 1151–1159.
[41] M. J. Goodwin, J. C. Dickenson, A. Ripak, A. M. Deetz, J. S. McCarthy, G. J. Meyer, L. Troian-Gautier *Chem. Rev.* **2024**, *11*, 7379–7464.
[42] S. Neumann, C. Kerzig, O. S. Wenger *Chem. Sci.* **2019**, *10*, 5624−5633.
[43] A. Aydogan, R. E. Bangle, A. Cadranel, M. D. Turlington, D. T. Conroy, E. Cauët, M. L. Singleton, G. J. Meyer, R. N. Sampaio, B. Elias, L. Troian-Gautier *J. Am. Chem. Soc.* **2021**, *38*, 15661–15673.
[44] T. Entradasa, S. Waldrona, M. Volk *J. Photochem. Photobiol. B* **2020**, *204,* 111787.
[45] W. Zhou, S. Wu, P. Melchiorre *J. Am. Chem. Soc.* **2022**, *144*, 20, 8914–8919.
[46] K. F. Biegasiewicz, S. J. Cooper, X. Gao, D. G. Oblinsky, J. H. Kim, S. E. Garfinkle, L. A. Joyce, B. A. Sandoval, G. D. Scholes, T. K. Hyster *Science* **2019**, *364*, 1166–1169.
[47] F. Felix, J. Ferguson, H.U. Güdel, A. Ludi *Chem. Phys. Lett.* **1979**, *62*, 153–157.
[48] P. Dongare, B. D.B. Myron, L. Wang, D. W. Thompson, T. J. Meyer *Coord. Chem. Rev.* **2017**, *345,* 86–107.
[49] M. Nakajima, S. Nagasawa, K. Matsumoto, T. Kuribara, A. Muranaka, M. Uchiyama, T. Nemoto *Angew. Chem. Int. Ed.* **2020,** *59,* 6847–6852.
[50] S. Amemori, Y. Sasaki, N. Yanai, N. Kimizuka *J. Am. Chem. Soc.* **2016**, *28*, 8702–8705.
[51] P. P. Lainé, F. Bedioui, F. Loiseau, C. Chiorboli, S. Campagna *J. Am. Chem. Soc.* **2006**, *23*, 7510–7521.
[52] T. Kinoshita, J. Fujisawa, J. Nakazaki, S. Uchida, T. Kubo, H. Segawa *J. Phys. Chem. Lett.* **2012**, *3*, 394–398.
[53] Z. Yuan, J. He, Z. Mahmood, L. Xing, S. Ji, Y. Huo, H.-L. Zhang *Dyes and Pigments,* **2022**, *199*, 110049.
[54] Y. Wei, Y. Li, M. Zheng, X. Zhou, Y. Zou, C. Yang *Adv. Optical Mater.* **2020,** *8*, 1902157.
[55] D. Liu, Y. Zhao, Z. Wang, K. Xua, J. Zhao *Dalton Trans.* **2018**, *47*, 8619−8628.
[56] Y .Sasaki, S. Amemori, N. Kouno, N. Yanai, N. Kimizuka *J. Mater. Chem. C*. **2017**, *5*, 5063−5067.
[57] G. A. Crosby, J. N. Demas *J. Am. Chem. Soc.* **1971**, *12*, 2841–2847.
[58] N. Sinha, C. Wegeberg, D. Häussinger, A. Prescimone, O. S. Wenger *Nat. Chem.* **2023**, *15*, 1730–1736.

TOC